

Effect of Butanol and Propylene Glycol in Amorphous MnO₂ Nanoparticles

Johnson HENRY¹, Kannusamy MOHANRAJ^{1,*}, Selvaraj KANNAN¹,
Seshathri BARATHAN² and Ganesan SIVAKUMAR³

¹Department of Physics, Manonmaniam Sundaranar University, Tirunelveli, Tamil Nadu 627012, India

²Department of Physics, Annamalai University, Annamalai Nagar, Tamil Nadu 608002, India

³CISL, Department of Physics, Annamalai University, Annamalai Nagar, Tamil Nadu 608002, India

(* Corresponding author's e-mail: kmohanraj.msu@gmail.com)

Received: 28 January 2013, Revised: 1 March 2013, Accepted: 14 February 2014

Abstract

Amorphous MnO₂ are synthesized using KMnO₄, butanol, and propylene glycol in an aqueous solution by using the precipitation method, under ambient conditions. The structure, molecular vibrations, surface morphological and optical properties of MnO₂ powders are studied using XRD, FTIR, SEM and UV-vis spectroscopy. From the XRD patterns, it is clear that both butanol and propylene glycol assisted MnO₂ particles are amorphous in nature. While the strong peak is noticed at 1384 cm⁻¹ in the FTIR spectra, which is due to the characteristic peak of MnO₂. SEM photographs show spherical shapes of MnO₂ particles, and the average size of a particle is about 200 nm for butanol assisted samples and is around 500 nm for propylene glycol assisted samples. Butanol assisted MnO₂ particles exhibit higher optical absorption in the visible region than propylene glycol. However, the estimated optical band gap of both the samples is found around 2.33 eV.

Keywords: MnO₂, butanol, propylene glycol, XRD, optical absorption

Introduction

Nanostructured transition metal oxides, which exhibit pseudocapacitance behavior, are considered to be excellent materials in terms of achieving high specific capacitance in hybrid supercapacitors. Manganese oxides are currently under extensive investigations because of their physical and chemical properties and wide technological applications, such as catalysts, electrode materials, sensor, ion-exchanging materials, energy transformation, molecular adsorption, magnetic materials, electrochromic materials, molecular sieves etc. Amorphous MnO₂ has been considered to be the most attractive electrode material for electrochemical capacitors due to its abundance, environmental friendliness, low cost, and favorable pseudocapacitive characteristics, more than noble metal oxides and other transition metal oxide systems [1,2]. Previously various approaches have been made to fabricate manganese dioxide, such as the drop-feeding method [1], ultrasonic method [2], hydrothermal method [3-5], precipitation method [6-9], solvothermal method [10] and microwave assisted hydrothermal method [11-13], using single precursor KMnO₄ with various acids such as HNO₃, H₂SO₄ and HCl and alcohols such as ethanol, methanol, pentanol, isopropanol, ethylene glycol and glycerol as reducing agents. It is understood that, from the above techniques, MnO₂ nanoparticles are formed, and are always amorphous in nature, when single precursor KMnO₄ is used with either acid or alcohols. After observing related work at a national and international level, there are no reports to be found to prepare MnO₂ particles using single precursor KMnO₄ with butanol and propylene glycol alcohols by the precipitation method. Hence, the objective of the work is to prepare MnO₂ by the precipitation method, using single precursor KMnO₄, with butanol

and propylene glycol alcohol as reducing agents. It is well known that the precipitation method is simple and low cost among the above experimental methods.

Materials and methods

In a typical synthesis, 0.5 g of KMnO₄ was dissolved in 30 ml de-ionized water, and 10 ml of butanol was added instantly, drop by drop, into the solution at room temperature. Within a few minutes, the mixture solution formed brown precipitate that indicated that the nucleation and crystallisation process had started in the solution. Finally, the precipitate was filtered using whatman filter paper, washed with ethanol and de-ionized water several times, and dried at room temperature. Similarly, 10 ml of propylene glycol was added drop by drop into 0.5 g of KMnO₄ solution (30 ml). Instantly, brown precipitate was formed. The obtained precipitate was properly washed and dried as per that of the butanol assisted sample.

The structural, molecular vibrations, surface morphological and optical properties of the MnO₂ powders were characterized by using XRD (X-Ray Diffraction), FTIR (Fourier Transform Infrared Spectroscopy), a SEM (scanning electron microscope) and UV-vis spectroscopy. The XRD measurements were performed by a PANalytical XPERT PRO diffractometer, with the Cu K α monochromatic radiation source ($\lambda = 1.5406\text{\AA}$) in the range of $2\theta = 10^\circ - 80^\circ$. Molecular vibration characteristics of the MnO₂ particles were carried out using Perkin Elmer FTIR spectrometer (Model RX-I) in the wavelength range of 4000 - 400 cm⁻¹. SEM micrographs were recorded for the above samples using JEOL SEM model, JEM -5610 LV with an accelerating voltage of 20 kV, at high vacuum (HV) mode and Secondary Electron Image (SEI). The SEI showed the fine surface clearly. Optical absorption characteristics of the MnO₂ particles were recorded using a JASCO UVVIDEC - 650 UV-Vis spectrophotometer.

Results and discussion

Figure 1 shows the X-ray diffractographs of both butanol and propylene glycol assisted MnO₂. In both the XRD patterns, MnO₂ particles exhibit broad reflections around $2\theta = 37^\circ, 56^\circ$ and 65° , which are due to a poorly crystalline nature (JCPDS no. 44-0141). The formation of poor-crystalline particles is due to either butanol or propylene glycol reacting with KMnO₄, yielding MnO₂ particles instantly. Therefore, the particles have a short-range crystallographic structure. The observed results are well in agreement with earlier reports [6,10,14]. The amorphous phase of MnO₂ is believed to be a good electrode material for pseudocapacitors [15]. However, an additional peak is found at $2\theta = 44.2^\circ$ in the propylene glycol assisted pattern, due to the presence of Mn₃O₄ (JCPDS no. 13-0162); perhaps the product is formed during the washing of the MnO₂ particles with ethanol. The result is also in good agreement with the earlier report by Han *et al.* [1] and Wang *et al.* [9].

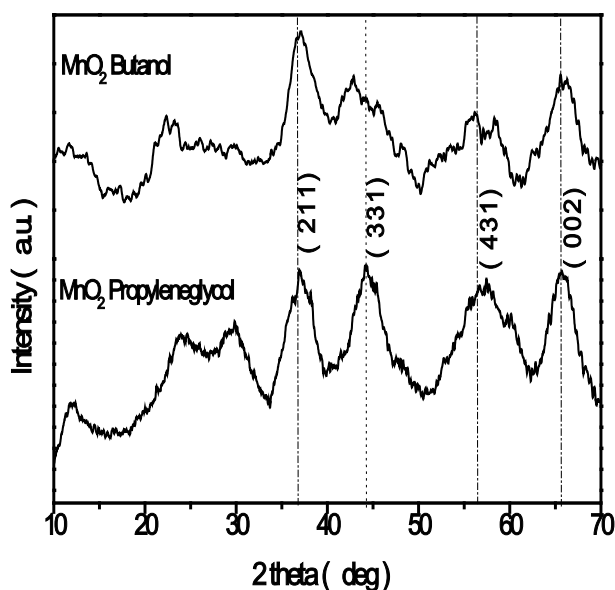


Figure 1 XRD pattern of MnO₂ particles.

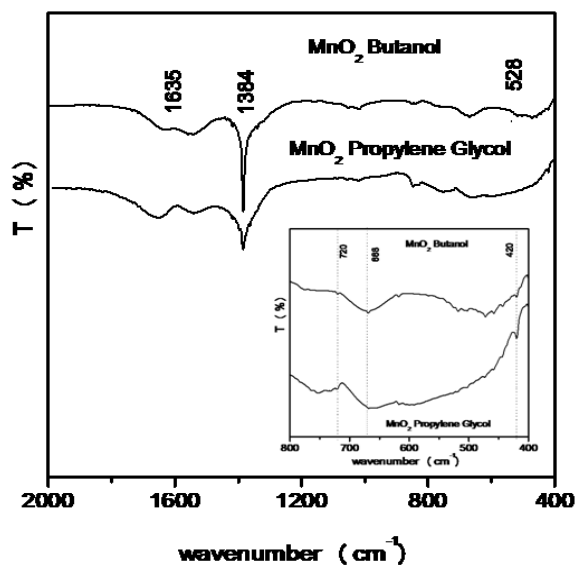


Figure 2 FTIR spectra of MnO₂ particles.

The FTIR Spectra of both butanol and propylene glycol assisted MnO₂ particles are shown in **Figure 2**. In the FTIR spectra of the butanol assisted sample, a band appears at 1635 cm⁻¹ and a sharp peak is seen at 1384 cm⁻¹, which is due to interaction of Mn with OH, O, H⁺ and K⁺. The water molecules, or cations, are intercalated into the MnO₂ interlayer, or tunnels are introduced during the synthesis to build the structures. The peak at 1280 cm⁻¹ shows a higher wavelength shift due to a strong bonded nature when compared to the earlier literature [11]. The authors have obtained the characteristic

peak of MnO₂ at 1280 cm⁻¹. Also, a weak band is observed at 528 cm⁻¹, which is attributed to Mn-O vibrations of MnO₂ [16], and some humps are detected around 720 cm⁻¹, 668 cm⁻¹ and 420 cm⁻¹ (which are shown in the insert of **Figure 2**), due to the bending vibrations of either birnessite-type MnO₂ or α-MnO₂ [11] that may be formed as by product during synthesis. Also, two broad bands at 619 cm⁻¹ and 475 cm⁻¹ are seen in the spectrum, which is due to Mn-O stretching vibrations [17]. Similar results are true in the propylene glycol assisted sample. However, the peak at 1384 cm⁻¹ is less intense when compared to the butanol assisted sample.

In order to determine the particle size, crystal habit, and morphology, SEM imaging is used. **Figure 3** shows SEM images of MnO₂ particles. The butanol assisted samples are very small in size, smaller than the propylene glycol assisted samples, spherical, with agglomeration free particles dispersed evenly on the surface of both images. The average sizes of the MnO₂ particles are found around 200 nm and 500nm for butanol and propylene glycol assisted samples respectively.

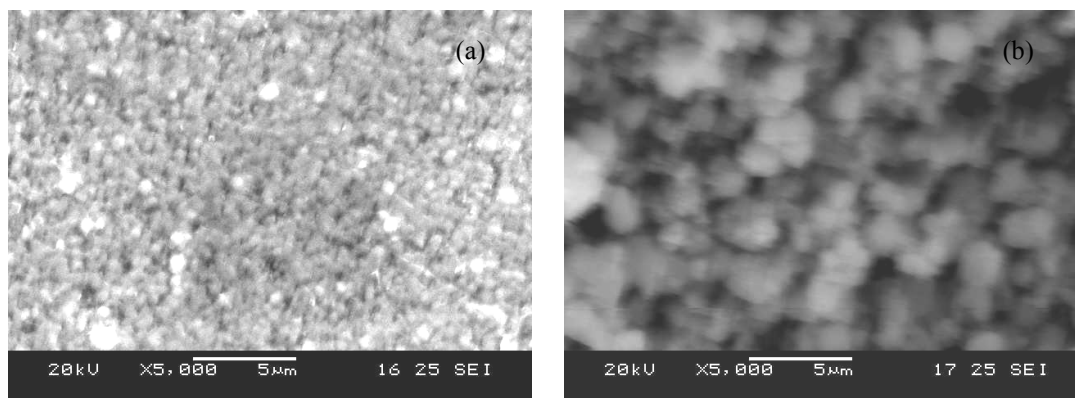


Figure 3 SEM images of MnO₂ particles prepared by using (a) butanol and (b) propylene glycol.

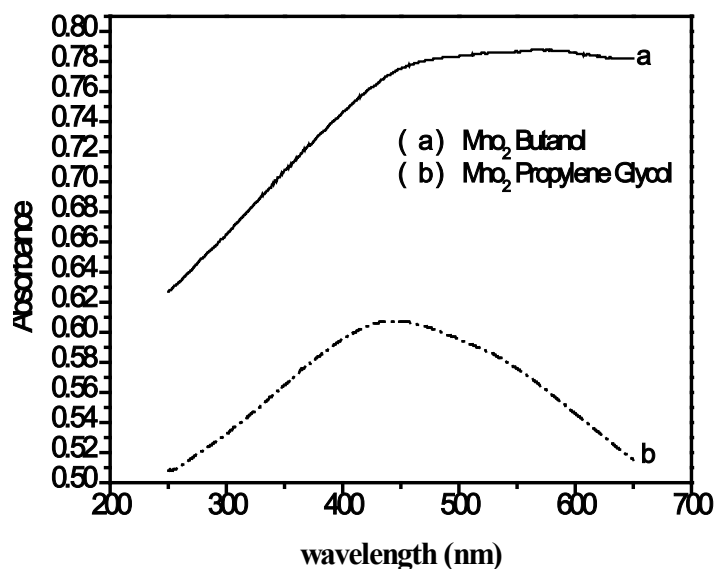


Figure 4 UV-VIS absorption spectrum of MnO₂ particles.

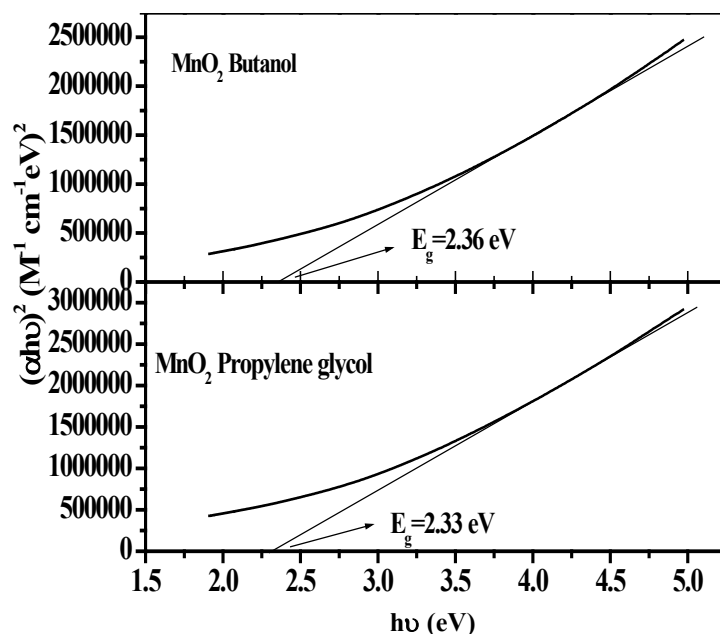
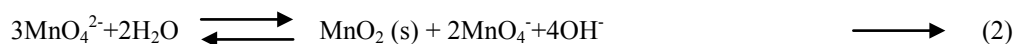


Figure 5 Plot of $(\alpha hv)^2$ Vs $h\nu$.

UV-vis absorption spectra of MnO₂ particles are shown in **Figure 4**. The butanol assisted MnO₂ particles have higher optical absorption in the visible region than the propylene glycol assisted samples. The maximum optical absorption is found around 460 nm for butanol and is 425 nm for propylene glycol. The observed maximum absorption value gradually decreased in the visible region. This result is in good agreement with the earlier report by Dang *et al.* [18].

To determine the optical band gap, the following dependence of α on photon energy was used $\alpha (h\nu - E_g)^n$ where E_g is band gap; α is absorption coefficient; n is an index that can assume values of (1/2, 2), depending on the nature of electronic transitions. For the direct allowed transitions, n has a value of 1/2, while for indirect allowed transitions $n = 2$. The optical band gaps for direct transitions are evaluated from the plot of $(\alpha hv)^2$ Vs $(h\nu)$ (**Figure 5**). The plot for direct transitions shows a straight line, and yields a value in the range 2.33 eV. The observed result fits well with the earlier reports of thin MnO₂ films prepared by Asogwa [19] and Sakai *et al.* [20].

Using organic reducing agents allows one to follow the reaction experimentally. This simple reaction takes advantage of one of the oldest known synthetic organic reactions—the use of KMnO₄ to oxidize unsaturated and functionalized organic molecules. In accordance with what is known about permanganate oxidations in organic chemistry, soon after addition of the organic reductant, the purple color of permanganate gives way to the green color of the one-electron reduced manganate ion (MnO₄²⁻). The manganate ion is unstable in moderately alkaline solutions and is quickly disproportionate, leading to the precipitation of brown, amorphous, MnO₂ and additional MnO₄²⁻. In solutions of alcohols (butanol and propylene glycol), permanganate is easily reduced to form amorphous MnO₂ phase, and acetone is oxidized. The reaction occurs within a few minutes on the bench top at room temperature. The formation of MnO₂ is given as below as equation [21].



Conclusions

The following results are drawn from the experimental studies. From the XRD patterns, both butanol and propylene glycol assisted MnO₂ particles are found to be amorphous in nature. The FTIR result confirmed the presence of a characteristic peak of MnO₂ in both samples at 1384 cm⁻¹, and has a strong bonded structure. In the SEM analysis, MnO₂ particles are spherical shape and the average particle size is found around 200 nm and 500 nm for butanol and propylene glycol assisted samples respectively. The maximum optical absorption is found to be around 460 nm for butanol and is 425 nm for propylene glycol, and thereafter the observed maximum absorption value is gradually decreased in the visible region. Butanol assisted MnO₂ particles show higher optical absorption characteristics in the visible region than propylene glycol assisted samples. The band gap energy of the samples is around 2.33 eV for both samples. From the above results, it is concluded that the single precursor KMnO₄, with alcohol assisted samples, can produce amorphous MnO₂ particles. Therefore, the material is to be used as an electrode material for electrochemical capacitors.

Acknowledgements

The authors are thankful to the UGC-SAP, New Delhi, for providing financial support to the Department of Physics, Manonmaniam Sundaranar University, Tirunelveli, Tamil Nadu, India, and the Prof & Head, Department of Physics, Annamalai University for providing analytical instrumentation facilities. Also, the authors are thankful to the authorities of the Manonmaniam Sundaranar University, Tirunelveli, for providing the seed money for the project, to carry out the work.

References

- [1] X Han, F Zhang, Q Meng and J Sun. Preparation and characterization of highly activated MnO₂ nanostructure. *J. Am. Ceram. Soc.* 2010; **93**, 1183-6.
- [2] S Zhu, X Wang, W Huang, D Yan, H Wang and D Zhang. Growth of width-controlled nanowires MnO₂ from mesoporous carbon and investigation of their properties. *J. Mater. Res.* 2006; **21**, 2847-54.
- [3] X Duan, J Yang, H Gao, J Ma, L Jiao and W Zheng. Controllable hydrothermal synthesis of manganese dioxide nanostructures: shape evolution, growth mechanism and electrochemical properties. *CrystEngComm* 2012; **14**, 4196-204.
- [4] N Tang, X Tian, C Yang, Z Pi and Q Han. Facile synthesis of α-MnO₂ nanorods for high-performance alkaline batteries. *J. Phys. Chem. Solids* 2010; **71**, 258-62.
- [5] W Xiao, D Wang and XW Lou. Shape-controlled synthesis of MnO₂ nanostructures with enhanced electrocatalytic activity for oxygen reduction. *J. Phys. Chem. C* 2010; **114**, 1694-700.
- [6] V Subramanian, H Zhu and B Wei. Alcohol-assisted room temperature synthesis of different nanostructured manganese oxides and their pseudocapacitance properties in neutral electrolyte. *Chem. Phys. Lett.* 2008; **453**, 242-9.
- [7] Y Chen, C Liu, F Li and H Cheng. Preparation of single-crystal α-MnO₂ nanorods and nanoneedles from aqueous solution. *J. Alloy. Compd.* 2005; **397**, 282-5.
- [8] O Ghodbane, J Pascal and F Favier. Microstructural effects on charge-storage properties in MnO₂-based electrochemical supercapacitors. *Appl. Mater. Interface.* 2009; **1**, 1130-9.

- [9] YT Wang, AH Lu, HL Zhang and WC Li. Synthesis of nanostructured mesoporous manganese oxides with three-dimensional frameworks and their application in supercapacitors. *J. Phys. Chem. C* 2011; **115**, 5413-21.
- [10] W He, Y Zhang, X Zhang, H Wang and H Yan. Low temperature preparation of nanocrystalline Mn₂O₃ via ethanol-thermal reduction of MnO₂. *J. Cryst. Growth* 2003; **252**, 285-8.
- [11] Y Li, J Wang, Y Zhang, MN Banis, J Liu, D Geng, R Li and X Sun. Facile controlled synthesis and growth mechanisms of flower-like and tubular MnO₂ nanostructures by microwave-assisted hydrothermal method. *J. Colloid Interf. Sci.* 2012; **369**, 123-8.
- [12] KU Din, M Altaf and M Akram. The kinetics of oxidation of L-tryptophan by water-soluble colloidal manganese dioxide. *J. Disper. Sci. Tech.* 2008; **29**, 809-16.
- [13] Z Khan, SAA Thabaiti, AY Obaid and ZA Khan. MnO₂ nanostructures of different morphologies from amino acids-MnO₄⁻ reaction in aqueous solutions. *Colloid. Surface. B* 2010; **81**, 381-4.
- [14] S Zhang, W Liu, J Ma and Y Zhao. A facile low-temperature route for preparing monodisperse Mn₃O₄ nanopolyhedrons from amorphous MnO₂ nanoparticles. *NSTI-Nanotech* 2010; **1**, 555-8.
- [15] M Song, S Cheng, H Chen, W Qin, KW Nam, S Xu, XQ Yang, A Bongiorno, J Lee, J Bai, TA Tyson, J Cho and M Liu. Anomalous pseudocapacitive behavior of a nanostructured, mixed valent manganese oxide film for electrical energy storage. *Nano Lett.* 2012; **12**, 3483-90.
- [16] P Zhang, X Li, Q Zhao and S Liu. Synthesis and optical property of onedimensional spinel ZnMn₂O₄ nanorods. *Nanoscale Res. Lett.* 2011; **6**, 1-8.
- [17] T Athar, N Topnani, A Hakeem and W Ahmed. Synthesis and characterization of MnO₂ and CdO nanoparticles. *Adv. Sci. Lett.* 2012; **5**, 1-4.
- [18] TD Dang, M A Cheney, S Qian, S W Joo and BK Min. A novel rapid one-step synthesis of manganese oxide nanoparticles at room temperature using Poly(dimethylsiloxane). *Ind. Eng. Chem. Res.* 2013; **52**, 2750-3.
- [19] PU Asogwa. Effect of deposition medium on the optical and solid state properties of annealed MnO₂ thin films. *J. Optoelectron Biomed. Mater.* 2010; **2**, 109-17.
- [20] N Sakai, Y Ebina, K Takada and T Sasaki. Photocurrent generation from semiconducting manganese oxide nanosheets in response to visible light. *J. Phys. Chem. B* 2005; **109**, 9651-5.
- [21] BJ Liddle, SM Collins and BM Bartlett. A new one-pot hydrothermal synthesis and electrochemical characterization of Li_{1+x}Mn_{2-y}O₄ spinel structured compounds. *Energy Environ. Sci.* 2010; **3**, 1339-46.